Electronic Supplementary Material (ESI) for Journal of Materials Chemistry A.

Supporting Information

Cu/M:ZnO (M = Mg, Al, Cu) Colloidal Nanocatalysts for the Solution Hydrogenation of Carbon Dioxide to Methanol

Alice. H. M. Leung,[a] Andrés García-Trenco,[a] Andreas Phanopoulos,[a] Anna Regoutz,[b] Manfred Erwin Schuster,[c] Sebastian D. Pike,[a] Milo S. P. Shaffer *[bd] and Charlotte K. Williams *[a]

[a] *Chemistry Research Laboratory, University of Oxford, 12 Mansfield Road, Oxford, UK OX1 3TA.*
[b] *Department of Materials, Imperial College London, London, UK SW7 2AZ.*
[c] *Johnson Matthey Technology Centre -Blount's Court, Sonning Common, UK RG4 9NH.*
[d] *Department of Chemistry, Imperial College London, London, UK SW7 2AZ.*

Corresponding author email: c.k.williams@imperial.ac.uk and m.shaffer@imperial.ac.uk

Index

M:ZnO@DOPA	Dopant source	Doping reagent added	Yield [a] (%)
Mg:ZnO@DOPA	Mg(^{n}Bu)(^{s}Bu) (0.7 M in hexane)	0.246 mL	87
Al:ZnO@DOPA	$AlEt_3$	19 mg	89
Cu:ZnO@DOPA	CuMes	31 mg	92

[a] Yields were calculated based on Zn content.

Table S1. Table showing the amount of doping reagent added to target 5 mol % doping in *M:ZnO@DOPA*.

M:ZnO@DOPA	EA (wt. %)			TGA (wt. %)	Estimated M:ZnO/DOPA
	C	H	Phosphinate [a]	Residual	
Mg:ZnO@DOPA	25.96	5.09	39.08	69.1	5.6
Al:ZnO@DOPA	24.46	5.11	36.84	74.5	5.8
Cu:ZnO@DOPA	24.57	4.57	37.00	70.9	5.9

[a] Inferred from carbon and hydrogen EA values

Table S2. Table showing the weight percentage of carbon and hydrogen obtained from EA, the residual mass from TGA and the estimated ratio between M:ZnO and the ligand for **Mg:ZnO@DOPA**, **Al:ZnO@DOPA** and **Cu:ZnO@DOPA**.

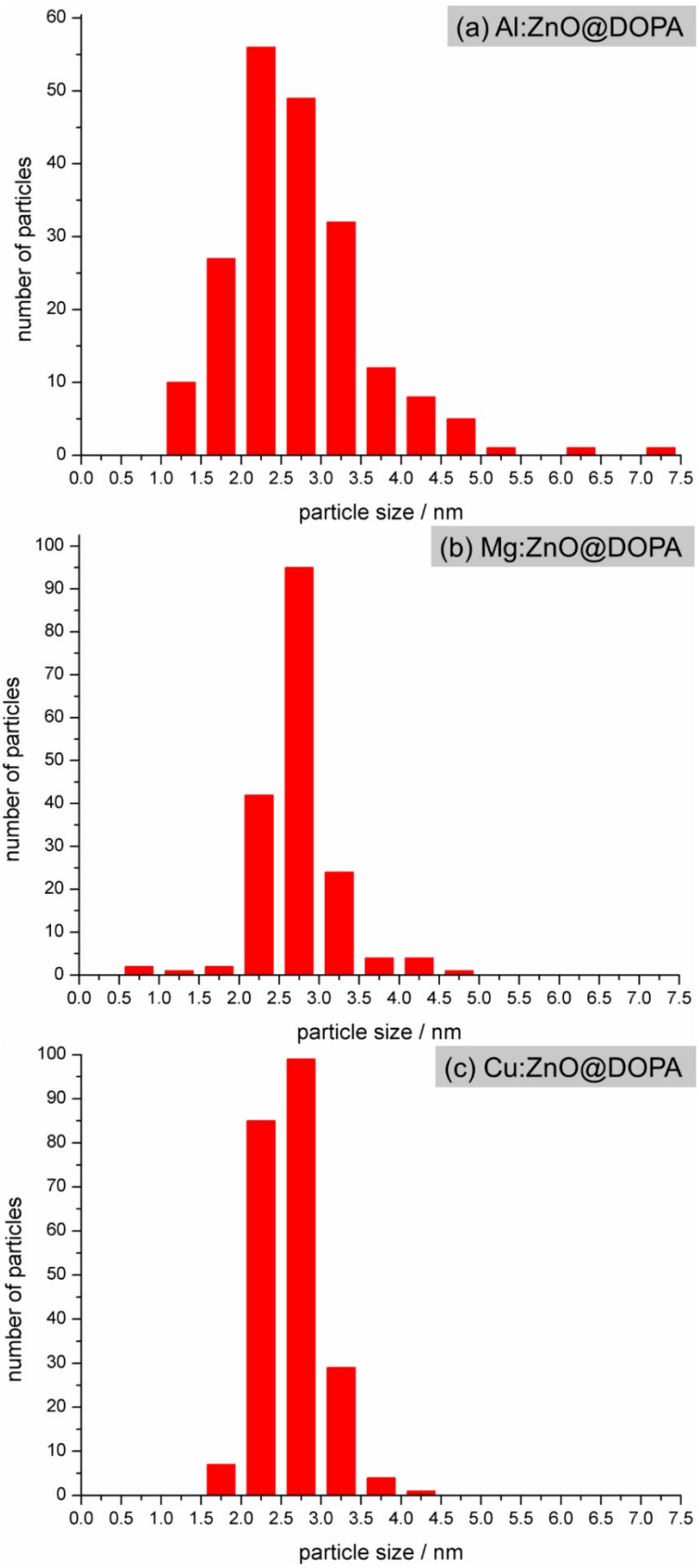

Figure S1. Particle size distribution, obtained from TEM analysis (see Figure 1e–f), of (a) **Al:ZnO@DOPA**, (b) **Mg:ZnO@DOPA** and (c**) Cu:ZnO@DOPA**.

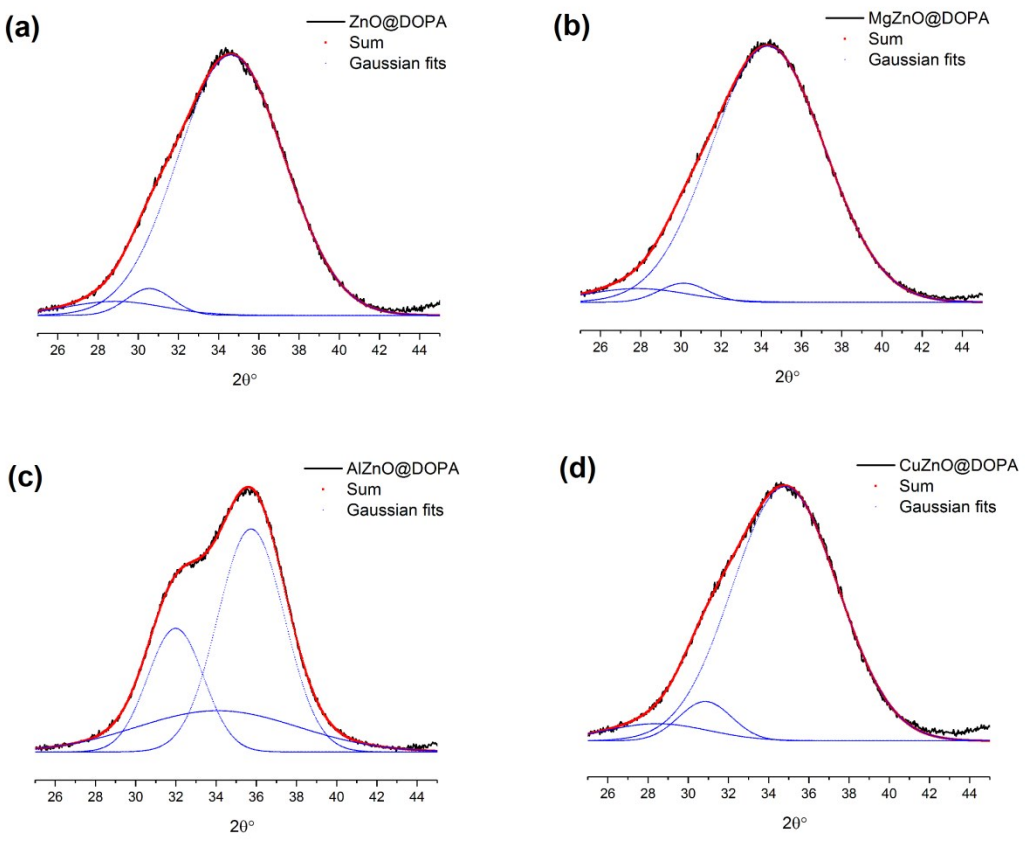

Figure S2. Gaussian fits applied to the XRD peaks in the range of 30–35° 2θ to determine the position of (101) facets for (a) **ZnO@DOPA**, (b) **Mg:Zno@DOPA**, (c) **Al:ZnO@DOPA** and (d) **Cu:ZnO@DOPA**.

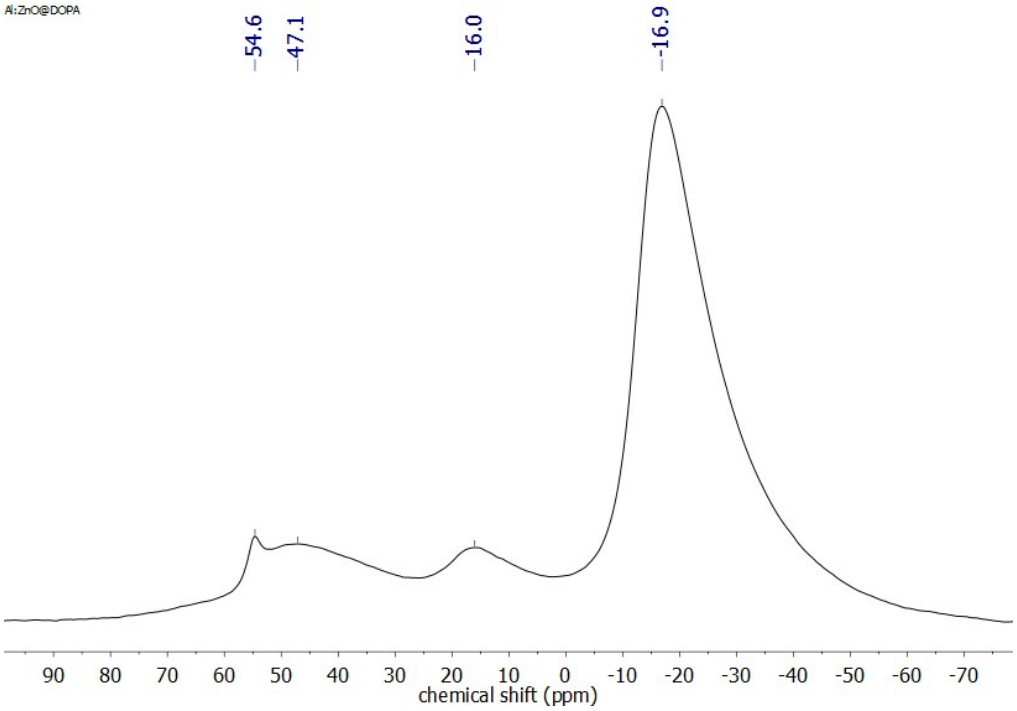

Figure S3. ^{27}Al-MAS-NMR spectrum **of Al:ZnO@DOPA**. Peak at δ +54.6 ppm indicates the presence of tetrahedral Al in the sample, δ +47.1 ppm for pentahedral Al and δ +16.0 & -16.9 ppm for octahedral Al.

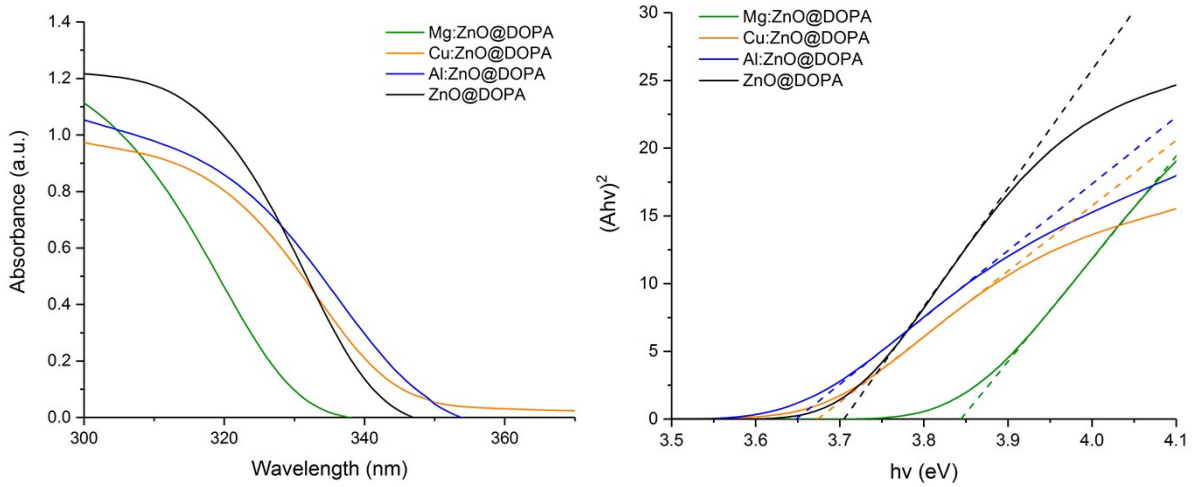

Figure S4. Optical spectroscopy spectra for **ZnO@DOPA** and *M:ZnO@DOPA*, including (a) UV-Vis spectra and (b) Tauc plots of **ZnO@DOPA** (black), **Mg:ZnO@DOPA** (green), **Al:ZnO@DOPA** (blue) and **Cu:ZnO@DOPA** (orange).

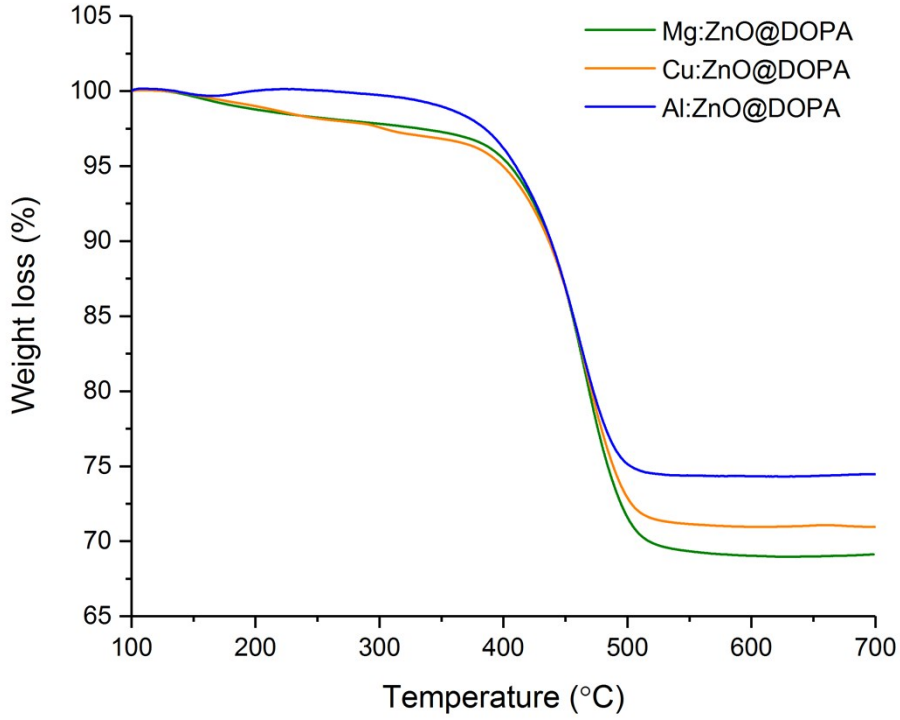

Figure S5. TGA profiles of **Mg:ZnO@DOPA** (green), **Al:ZnO@DOPA** (blue) and **Cu:ZnO@DOPA** (orange), from 100–600 °C, with ramp rate of 5 °C/min and under a flow of N_2 (60 mL min^{-1}).

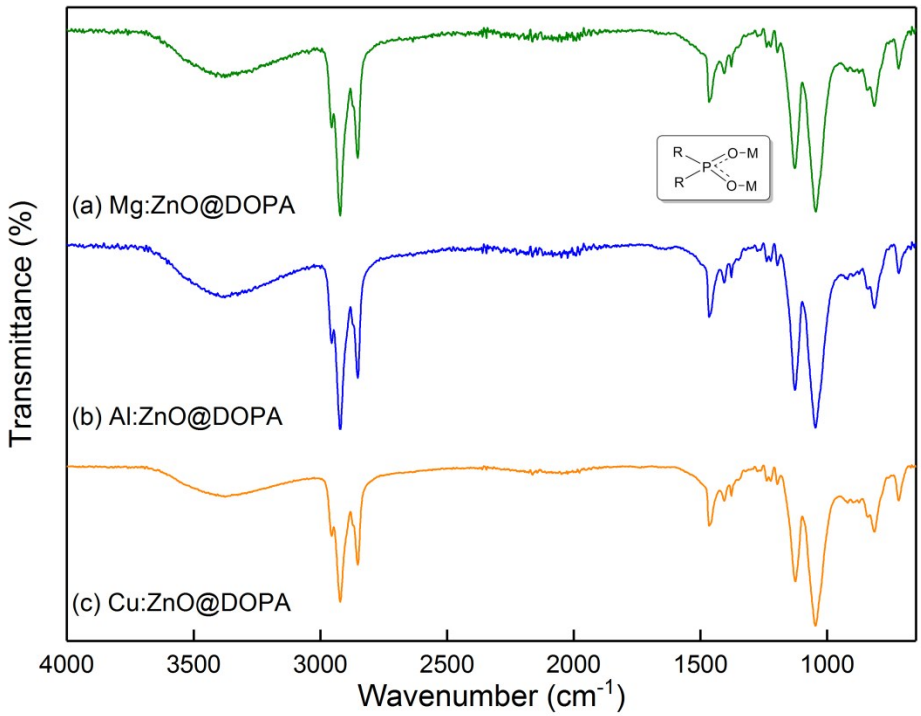

Figure S6. FT-IR spectra of (a) **Mg:ZnO@DOPA**, (b) **Al:ZnO@DOPA** and (c) **Cu:ZnO@DOPA**, with the inset figure showing the coordination mode of $[DOPA]^-$ on the nanoparticle surface.

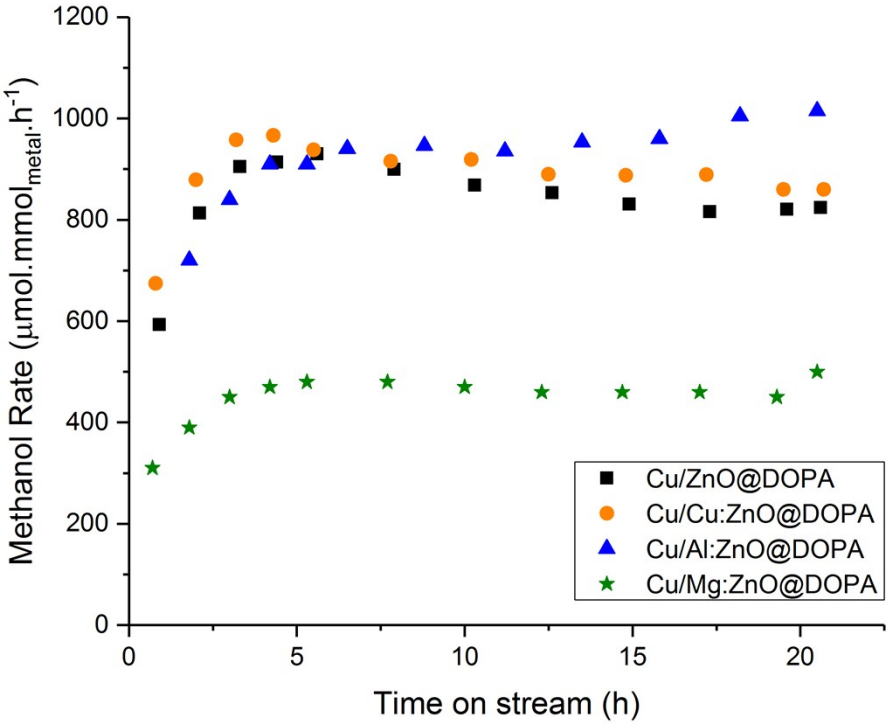

Figure S7. The methanol production rates of the tested colloidal Cu/ZnO nanocatalysts in the hydrogenation of CO_2 over 20 h time-on-stream (210 °C, 50 bar CO_2:H_2 1:3, 150 mL min^{-1}).

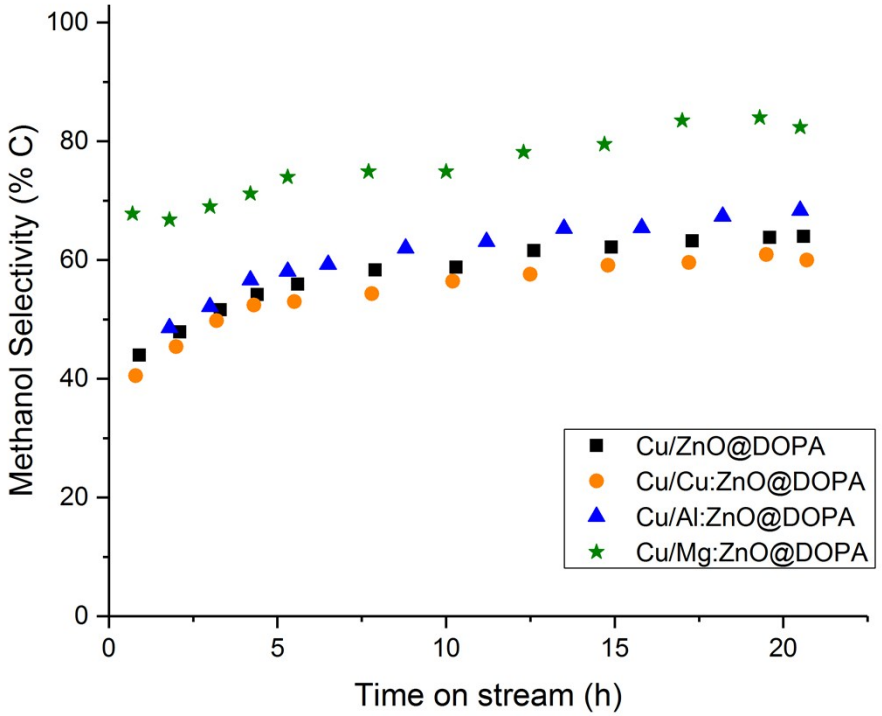

Figure S8. The methanol selectivity of the tested colloidal Cu/ZnO nanocatalysts in the hydrogenation of CO_2 over 20 h time-on-stream (210 °C, 50 bar CO_2:H_2 1:3, 150 mL min^{-1}). The only other product produced from the reaction is CO (generated by rWGS reaction).

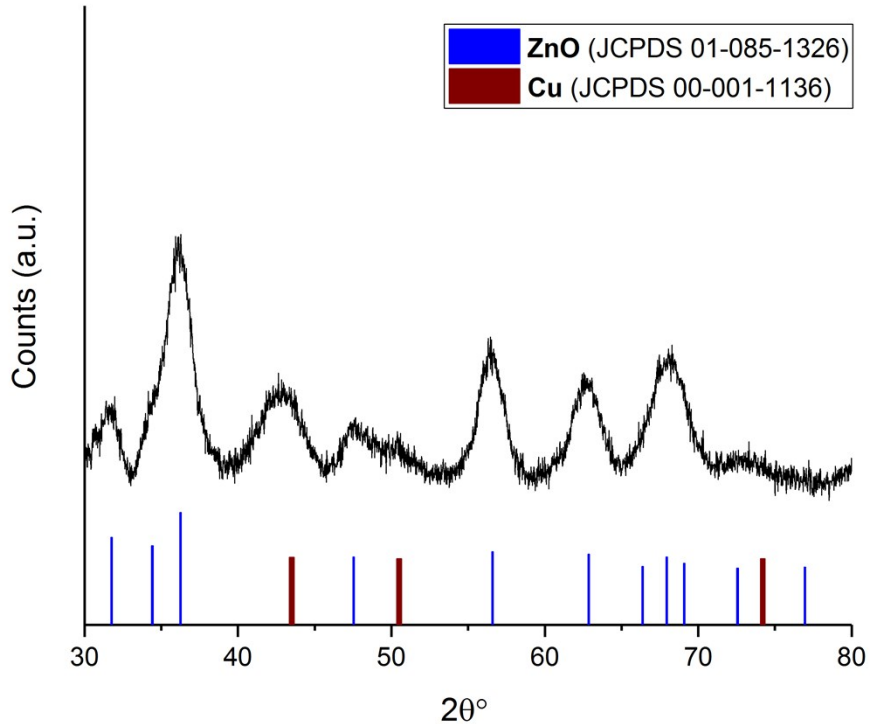

Figure S9. Powder XRD pattern of the post-catalysis sample of **Cu/Mg:ZnO@DOPA**. Reference bars: ZnO (blue, JCPDS 01-085-1326), Cu (brown, JCPDS 00-001-1136).

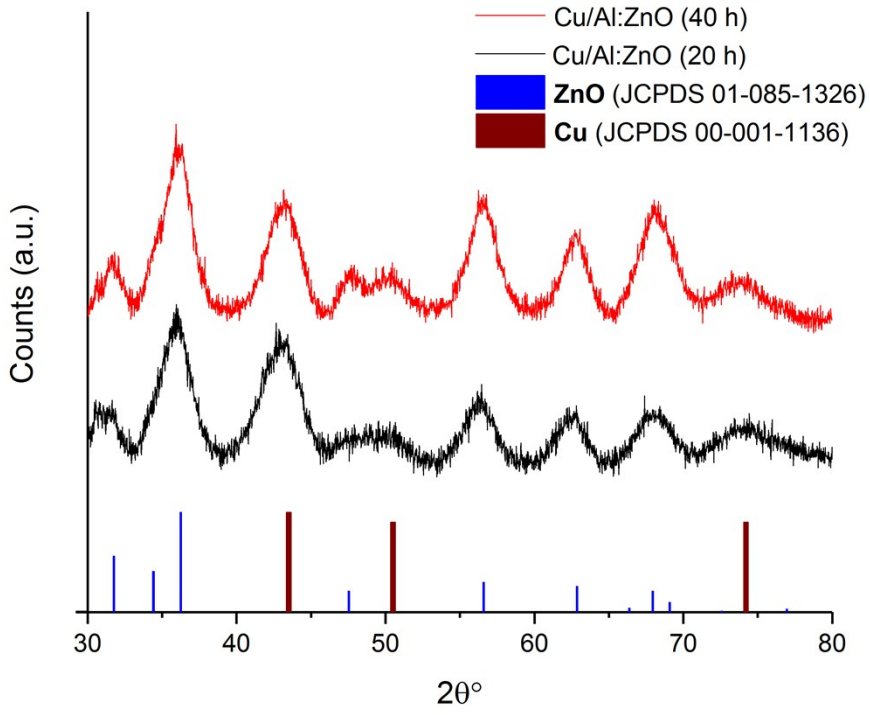

Figure S10. Powder XRD patterns of the post-catalysis sample of **Cu/Al:ZnO@DOPA** at 20 h time-on-stream (black) and 40 h time-on-stream (red). Reference bars: ZnO (blue, JCPDS 01-085-1326), Cu (brown, JCPDS 00-001-1136).

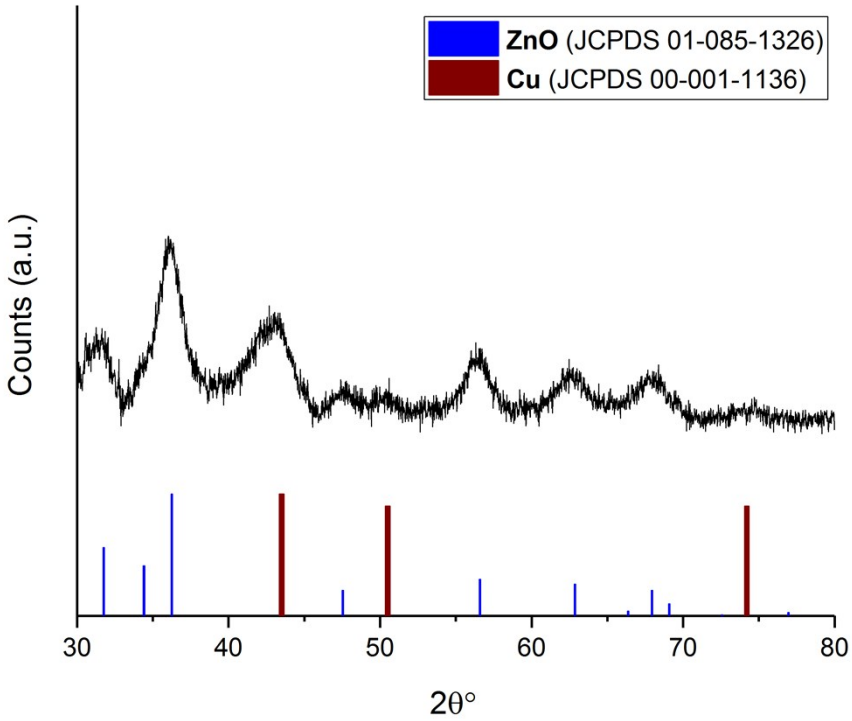

Figure S11. Powder XRD pattern of the post-catalysis sample of **Cu/Cu:ZnO@DOPA**. Reference bars: ZnO (blue, JCPDS 01-085-1326), Cu (brown, JCPDS 00-001-1136).

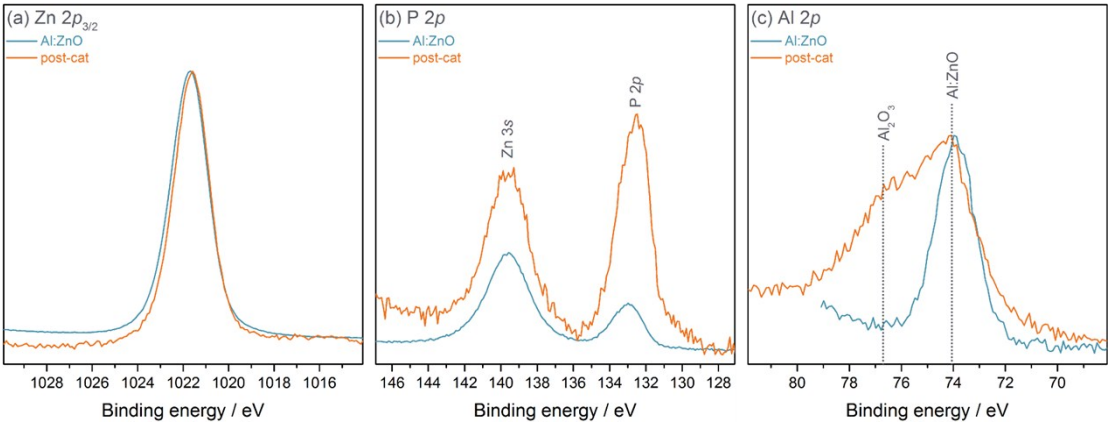

Figure S12. XPS spectra of post-catalysis sample of **Cu/Al:ZnO@DOPA** (orange) and pre-catalysis sample of **Al:ZnO@DOPA** (blue), with core lines of (a) Zn $2p_{3/2}$, (b) P 2*p* and (c) Al 2*p*. An extra species is observed in (c) Al 2*p* core line in the post-catalysis sample at a higher binding energy compared to the pre-catalysis sample.

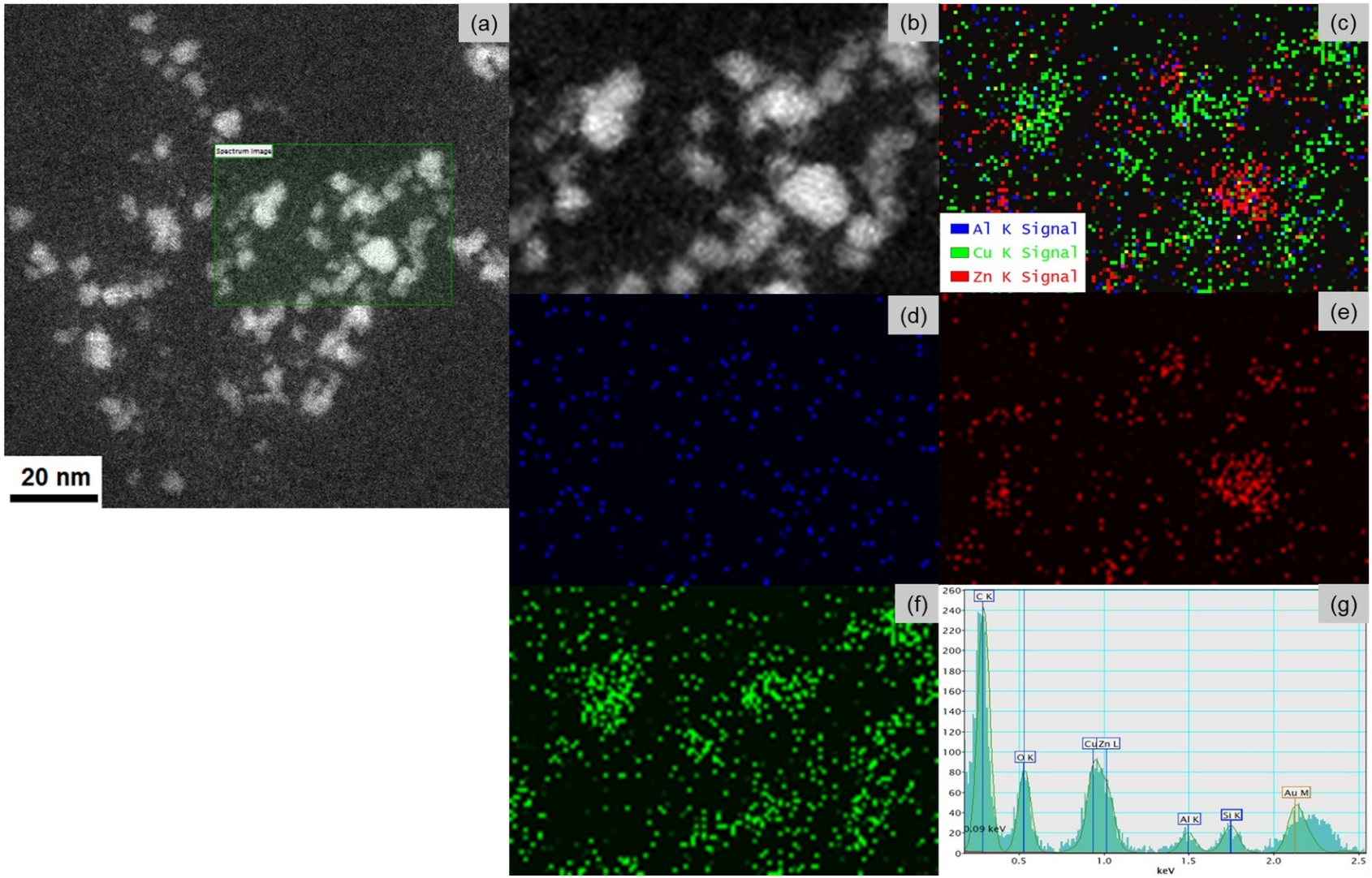

Figure S13. HAADF-STEM image (*a,b*) of post-catalysis sample of **Cu/Al:ZnO@DOPA**, along with EDX maps showing the location of aluminium (d), zinc (e) and copper (f). (c) Shows an RGB overlay of the Zn(red), Cu(green) and Al(blue) EDX maps; EDX spectra in (g) indicates the Al K peak used for fitting.

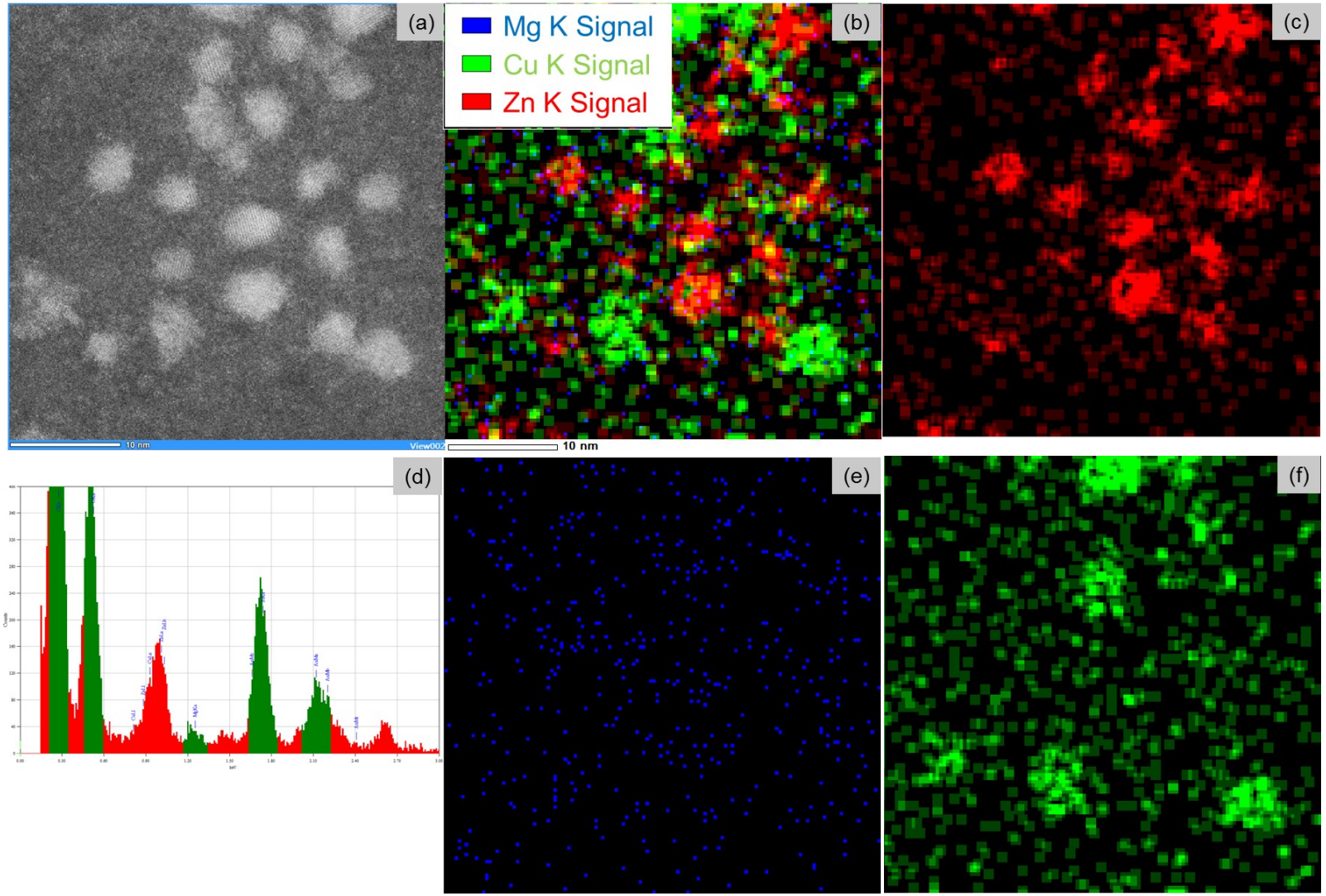

Figure S14. HAADF-STEM image (a) of post-catalysis sample of **Cu/Mg:ZnO@DOPA**, along with EDX maps showing the location of zinc (c), magnesium (e) and copper (f). (b) Shows an RGB overlay of the Zn(red), Cu(green) and Mg(blue) EDX maps; EDX spectra in (d) indicates the Mg K peak used for fitting.

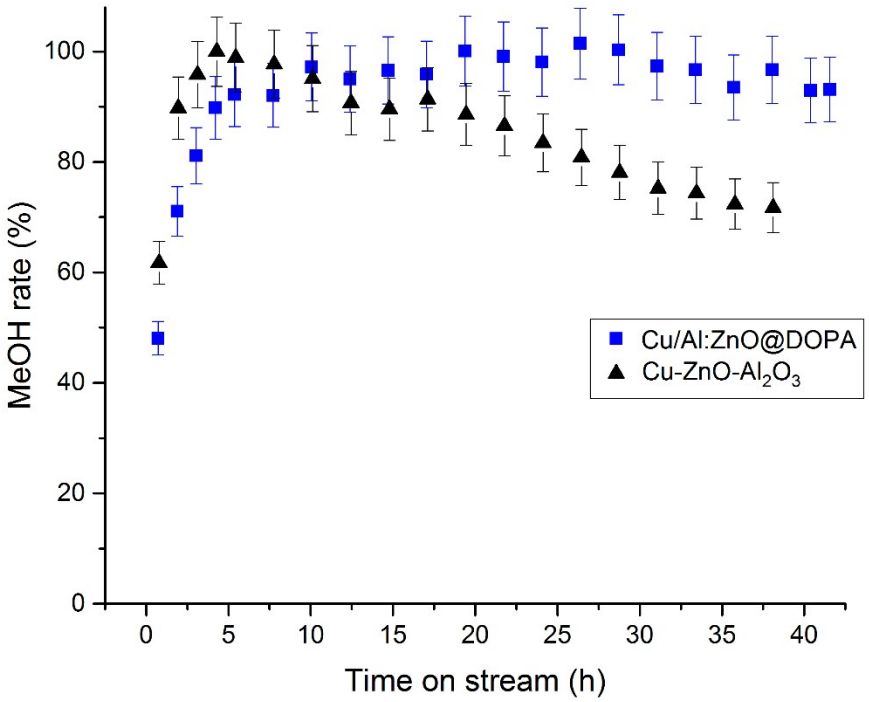

Figure S15. Percentage of catalyst deactivation of **Cu/Al:ZnO@DOPA** and commercial heterogeneous Cu-ZnO-Al_2O_3, over 40 h time-on-stream.

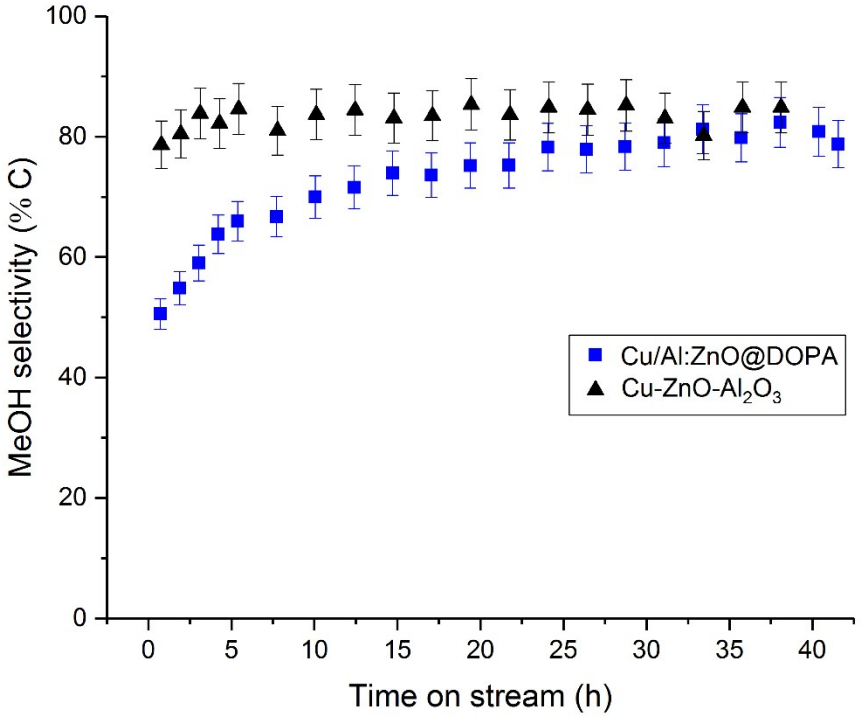

Figure S16. Methanol selectivity of **Cu/Al:ZnO@DOPA** and commercial heterogeneous Cu-ZnO-Al_2O_3, over 40 h time-on-stream.

Rationale for catalytic reaction conditions

Given the reaction parameters used during the catalytic experiments, there is expected to be no mass transport limitations. Several detailed studies of the mass transfer during the slurry phase hydrogenation of CO_2 revealed that "…the impeller speed, feed flow rate, and temperature had significant effects on the mass transfer coefficient".[1,2]

- In this study, the same impeller speed of 1500 r.p.m. as these previous studies was used, which was found to agitate the solvent sufficiently to ensure good gas-liquid mixing. Additionally, this study utilised a Parr gas entrainment impeller, which allows continuous recirculation of head space gas, through the impeller, directly into the liquid phase, truly maximising gas-liquid mixing.
- At feed flow rates of 1.9–3.7 mol h^{-1} (syngas), catalytic mixtures containing <6 wt% slurries (<5 g of catalyst per 100 mL) were shown to not limit the overall rate.[3] This study used flow rates of 150 mL min^{-1} (~20 mol h^{-1}) and 0.8 mmol (<100 mg) catalyst per 100 mL solvent. As these conditions fall well below the threshold for rate inhibition, it follows that the feed flow rates used in this study did not limit the mass transfer or overall rate.
- The temperature will affect the mass transfer due to the solubility of gases within the liquid, with higher temperatures making the gas less soluble. The temperatures used in this study were towards the lower end (210 °C) of temperatures more recently used for CO_2 hydrogenation using Cu-based catalysts (205–250 °C). In the detailed studies above, inert mineral oils (Witco 40 and Witco 70) are used. Although direct comparisons are not available on the solubility of gases in these oils compared to other non-aqueous solvents, it appears that the solubility of CO_2 in Witco 40[4] is at least comparable to CO_2 in toluene:[5]
    - Witco 40 (30 °C, 8 bar, mole fraction = 0.08)
    - Toluene (35 °C, 17 bar, mole fraction = 0.18)
- The nanoparticles used in this study are very small (<3 nm) compared to other catalysts used for this reaction, which are typically in the micrometer-regime. The system used in this study will, therefore, have no pore diffusional limitations, which can become significant for larger particle sizes.

With these data in mind, mass transfer will not limit the rate of reaction in the experimental set up and can be safely disregarded in the rate discussion.

[1] S. Lee and A. Sardesai, *Top. Catal.*, 2005, **32**, 197–207

[2] V. R. Parameswaran, M. R. Gogate, B. G. Lee and S. Lee, *Fuel Sci. Technol. Int.*, 1991, **9**, 695–744

[3] M. K. Ko, PhD thesis, University of Akron, 1987

[4] M. K. Ko, S. Lee and C. J. Kulik, *Energy & Fuels*, 1987, **1**, 211–216

[5] E. N. Lay, V. Taghikhani and C. Ghotbi, *J. Chem. Eng. Data*, 2006, **51**, 2197–2200